straint Stresses in Long Reinforced Slabs", Highway Research Board Proceedings, Vol. 33 (1954).
17. Highway Research Board Special Report 4, "Road Test One-MD", (1952).
18. B. F. FRIBERG, "Some Observations on the Use of Reinforcing Steel in Concrete Pavements", American Concrete Institute Proceedings, Vol. 47 (Sept. 1950).
19. H. M. WESTERGAARD, "Stresses in Concrete Pavements Computed by Theoretical Analysis", Public Roads, April 1926.
20. L. W. TELLER AND E. C. SUTHERLAND, "The Structural Design of Concrete Pavements", Public Roads, October 1935, November 1935, December 1935, September 1936, October 1936, April-May-June 1943.
21. H. D. CASHELL AND S. W. BENHAM, "Experiments with Continuous Reinforcement in Concrete Pavements", Highway Research Board Proceedings, Vol. 29 (1949).
22. B. F. FRIBERG, "Sector Analysis of Concrete Pavements, An Analysis of Pavement Load Stresses and Deflections", American Society of Civil Engineers (in course of Publication).
23. H. M. WESTERGAARD, "Analysis of Stresses in Concrete Roads Caused by Variations of Temperature", Public Roads, May 1927.

Velocity Distribution in a Street or Similar Channel

G. S. TAPLEY, *Civil Engineer*
Bureau of Engineering, City of Los Angeles

Manning's formula already has been applied to the determination of velocity distribution in the form $v = Gy^{2/3}$, where v is the velocity in a vertical element of water cross section, y is the depth of the element, and G is a constant depending on the roughness of channel surface and the channel slope. In the region affected by a curb or vertical side wall, however, this relationship gives irrational results, since the magnitude of velocity at the wall actually must be zero, whereas the equation above yields a finite value.

Differentiation of Manning's formula, on the other hand, gives an equation representing a locus of rational form for the region nearer the side wall. This locus and that of the equation given above, applied to the portion of the channel more remote from the side wall, forms a combined locus which agrees approximately with experimental results. The discrepancy is systematic, however, and is attributed to the neglected shear between water elements.

● FOR uniform flow in an open channel the gravitational and frictional forces are equal, so that

$$\tau PL = -wSLA^{1} \qquad (1)$$

where τ is the frictional drag per unit of area of channel surface, P is the wetted perimeter of water cross section, L is the length of channel, w is the weight of a cubic unit of water, S is the longitudinal slope of the channel, and A is the area of the water cross-section. From (1) it follows that the hydraulic radius R commonly employed in Manning's formula and elsewhere represents the ratio of unit drag to unit gravitational force; for, by (1)

$$R = \frac{A}{P} = -\frac{\tau}{wS}\,. \qquad (2)$$

[1] See for example, "Elementary Mechanics of Fluids," Rouse, p. 215.

In ordinary practice the hydraulic radius or "hydraulic mean depth" represents a whole cross section, and τ is uniform over the wetted surface. The velocity obtained by employing such an hydraulic radius in Manning's formula is then the mean velocity for the section,

$$V = \frac{1.486}{n} R^{2/3} S^{1/2}, \qquad (3)$$

where n is Manning's roughness coefficient. Or, for convenience

$$V = GR^{2/3}, \qquad (4)$$

where

$$G = \frac{1.486}{n} S^{1/2}. \qquad (5)$$

No distinction is ordinarily made in employing the formula as regards differences of shape of channel cross-section.

In a channel of infinite width and uniform depth in the cross-section the hydraulic radius becomes the depth y, and the velocity is given by

$$v = V = Gy^{2/3}, \qquad (6)$$

where v represents the velocity in any vertical element of the cross section. For a channel in which the depth varies very gradually from one side to the other of the cross section the horizontal velocity distribution for the portion unaffected by a side wall may be calculated by (6), using v, representing local velocities, or by

$$v = Gy^{2/3}, \qquad (7)$$

as for example, on pp. 149, 150[2]. Application of eq. (7) to a case where velocities vary transversely in a cross section is equivalent to neglecting water shear on the sides of the elements. Data following will show that neglect of water shear in a model street section yields an approximate velocity distribution which is accurate enough for many purposes, but which does involve an appreciable discrepancy.

Equation (7), when applied, on the other hand, to the portion of a channel wherein velocity distribution is affected by a vertical side wall or curb, gives irrational results, since in approaching the wall the velocity actually must approach zero, whereas the formula yields a finite velocity at the wall, depending only on the depth at that point. In many problems of highway drainage, and of other fields of hydraulics, the region of flow influenced by a side wall is an important one. It will be shown that Manning's formula can also be applied to the determination of approximate velocity distribution in this region. As in the portion of the channel to which eq. (7) is applicable, the neglect of shear on the lateral water boundary causes an appreciable discrepancy. The accuracy obtainable is considered satisfactory, however, in view of the various approximations usually involved in hydraulic calculations; for example, the approximation involved in the assumption that the 6th power of Manning's n represents a measure of roughness[3]. In the present application of Manning's formula, moreover, velocity distribution in the vertical is being neglected.

Since (2) is true for a whole channel, it

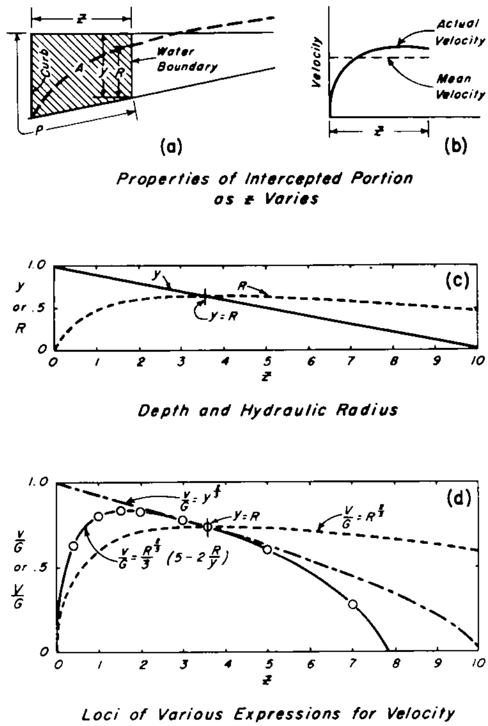

Figure 1

[2] "Hydraulics of Runoff from Developed Surfaces," by Carl F. Izzard, *Proceedings* Highway Research Board (1946 Annual Meeting).

[3] Engineering Hydraulics, Rouse, p. 115; or see [1].

should be equally true for a portion of a channel bounded on one side by a curb or side wall and on the other by a water boundary such as that shown in Figure 1(a), if the shear on the water boundary can be considered negligible. Thus let A and P represent the cumulative values for area and wetted (solid) perimeter between the side wall and the water boundary as z increases. Since Manning's formula for discharge,

$$Q = G\frac{A^{5/3}}{P^{2/3}}, \tag{8}$$

states, in effect, that discharge in different channels, regardless of shape of cross section, depends only on A and P, G being constant, it follows that in portions of a given channel, such as that in Fig. 1(a) the rate of change of Q as z varies is given by

$$\frac{dQ}{dz} = G\left[A^{5/3}\left(-\frac{2}{3}P^{-5/3}\frac{dP}{dz}\right) + P^{-2/3}\left(\frac{5}{3}A^{2/3}\frac{dA}{dz}\right)\right]. \tag{9}$$

Now, in (9)

$$\frac{dP}{dz} = 1, \tag{10}$$

practically, and

$$\frac{dA}{dz} = y \tag{11}$$

Hence, putting $A/P = R$, (9) becomes

$$\frac{dQ}{dz} = G\left(-\frac{2}{3}R^{5/3} + \frac{5}{3}yR^{2/3}\right), \tag{12}$$

or

$$\frac{dQ}{dz} = G\frac{R^{2/3}}{3}(5y - 2R) \tag{13}$$

Moreover, since

$$v = \frac{dQ}{y\,dz}, \tag{14}$$

the velocity at any value of z, by (13) and (14) is

$$v = G\frac{R^{2/3}}{3}\left(5 - 2\frac{R}{y}\right). \tag{15}$$

Note that when $R = y$, eq. (15) reduces to (4) so that the local velocity at the corresponding point must equal the mean velocity of the intercepted portion of the cross-section.

Referring again to Fig. 1(a) note that the cumulative value of R varies with z, as shown by the dashed locus, eventually becoming greater than the depth y. The relationship between the mean velocity, according to (4) and the actual velocity, for an intercepted portion of channel cross-section of width z, is illustrated in Fig. 1(b). "Actual velocity refers to the velocity in a vertical element, assuming no variation of velocity vertically.

APPLICATION OF VARIOUS EXPRESSIONS FOR VELOCITY DISTRIBUTION TO A THEORETICAL CHANNEL

Figures 1(c) and 1(d) were prepared to illustrate the application of various expressions for velocity distribution derived from Manning's formula. The channel represented in Fig. 1(c) is a triangular one, 1-ft. deep at the vertical side wall, 0-ft. deep at the outer edge, and 10-ft. wide. In Fig. 1(d) data representing eq. (15) showed that velocities become negative in the right-hand portion of the graph. According to eq. (15) negative values occur when R becomes greater than $5/2\ y$.

The left-hand portion of the graph of eq. (15) in Fig. 1(d), on the other hand, has a rational shape. The curve is tangent to the locus of eq. (7) at the point where $R = y$. The latter locus, in turn, has an irrational shape in its left-hand portion, since the indicated velocities at the curb are finite (in fact, maximum velocities occur there), whereas velocities at the curb must actually have zero magnitudes. The left-hand portion of the locus of eq. (15) and the right-hand portion of the locus of eq. (7), however, form a combined locus of rational shape, and one which, it will be shown later, agrees with measured velocities fairly well.

The third curve shown in Fig. 1(d) is the locus of eq. (4). This curve passes through the point of tangency of the other two curves; i.e., at the point where $R = y$. Note that at this point the maximum velocity is indicated by eq. (4), whereas the maximum for eq. (15) occurs nearer the curb, and has a higher value. Since eq. (4) represents uniform velocities in the intercepted portion of the cross section it

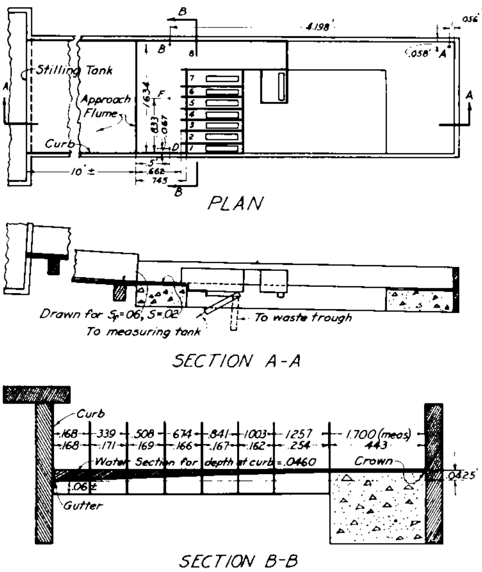

Figure 2

is not to be expected that the locus would indicate local velocities.

COMPARISON OF THEORETICAL AND EXPERIMENTAL VELOCITIES

Experimental data were obtained on a $\frac{3}{32}$-scale model of half of a 36-ft.-wide pavement with crown height = .45 ft.[4] The apparatus for measuring the flow distribution is illustrated in Fig. 2, and the crown section, together with the observed water surface, is shown in Fig. 3.

The experimental data represent a model flow, Q = .0992, and slope, S = .02; the observed water surface was used without averaging to a level surface. An average value of n = .0102, representing 9 runs involving 3 Q's on each of 3 different channel slopes was used to compute the value of G = 20.58 by eq. (5).

The three sets of data plotted in Fig. 4 represent cumulative values of Q as functions of z. As indicated by the legend Set 1 represents the experimental Q $(=\Sigma\Delta Q)$, set #2 the cumulative Q $(=GAR^{2/3})$, and set #3 the Q $(=G\Sigma\Delta zy^{5/3}{}_{\text{av}})$. It may be noted in Fig. 4 that set #2 agrees well with the experimental values in the left hand portion of the graph, but diverges considerably at the extreme right; the ratio of calculated to observed Q for the whole channel being .0835/.0992 = .842. Set #3 diverges appreciably from the experi-

[4] The apparatus is described in "Hydrodynamics of Model Storm Sewer Inlets Applied to Design" by G. S. Tapley, Transactions ASCE vol. 108 (1943) and, more fully in [5] "Depth and Distribution Data for Flow in Model Street," by G. S. Tapley (1941), a copy of which is on file in the Engineering Societies Library, 33 W. 39th St., New York, N. Y.

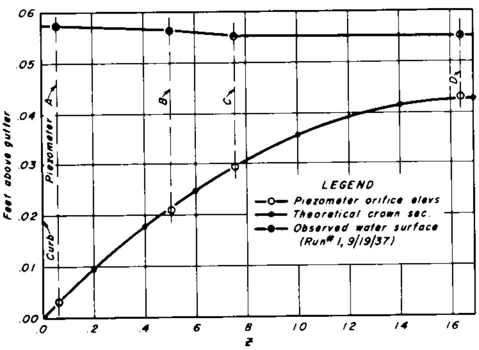

Figure 3

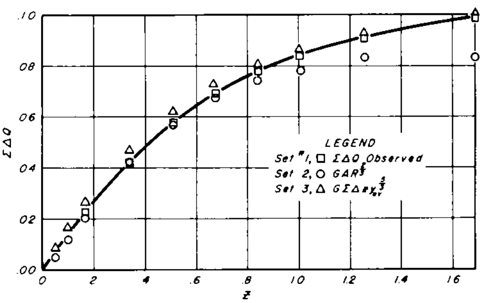

Figure 4

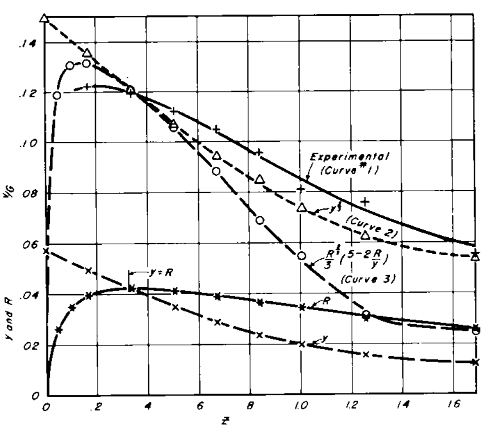

Figure 5

mental curve in the left-hand portion of the figure, the divergence being about 12 percent at the point $y = R$, but the discrepancy decreases in the right-hand portion to a small magnitude at the right-hand extreme. The values of y_{av} used in set #3 were taken at the centers of the increments of the channel width.

Figure 5 contains 3 curves representing values of v/G as functions of z for the same case as that used in Figures 3 and 4. Also shown at the bottom of Fig. 5 are curves of y and cumulative R. Values of v/G depend only on the geometrical properties of the water cross section in the case of curves #2 and 3, and on the scaled slopes of the experimental Q curve in Fig. 4 divided by yG in the case of curve #1. It may be observed in Fig. 5 that the combination of the left portion of curve #3 and the right portion of curve #2 yields a curve which agrees fairly well with the experimental curve, but that the right and left portions, respectively, are unreasonable in shape. It may particularly be noted that the experimental curve crosses the combined curve at about the point where $y = R$, and that there is an appreciable, and apparently systematic, discrepancy between the theoretical curve and the experimental one, the discrepancy being negative in one portion and positive in the other, evidently in conformity with the direction of the water shear to the left of, and to the right of the point of maximum velocity.

Results confirmatory of those shown in Fig. 5 were obtained from data representing the average of a large number of tests on the model represented by Fig. 5, and described in references #4 and 5. A level water surface in the cross section was determined in the averaging process. The data are omitted here in the interest of brevity.

DISCUSSION

Curtis L. Larson: *Assistant Professor of Agricultural Engineering, University of Minnesota*—This paper on the distribution of flow in a flat triangular channel is of special interest to the writer, having investigated the same problem at the St. Anthony Falls Hydraulic Laboratory in 1949.[1] As with Tapley, the need for such information was made evident by a previous study on the hydraulics of storm sewer inlets.[2]

One of the main conclusions of the study was that, where the depth of flow varies transversely at a rate of 5 percent (20:1) or less, the velocity in a vertical element is a function of the depth of flow except in the region near the curb. The Manning equation, with slight modification, was found suitable for expressing this relation. These findings are in agreement with those of Tapley.

The tests were performed in a concrete-lined channel having a variable cross-slope and a sloping curb. The curb was constructed so as to have a slope ratio of 2 to 1 when the cross-slope was zero. The concrete lining was made with a well-graded sand and received no finishing except for drawing a screed once across the surface. Experimental flow distributions were measured at an overfall by using a movable sampling device having vertical cutting edges. Theoretical distributions were developed by the use of the Manning equation in two-dimensional form. Using Tapley's notation

$$v = Gy^{2/3} \qquad (1)$$

where $G = 1.486\ S^{1/2}/n$. Accordingly, the Manning coefficient n was determined for two-dimensional flow by setting the cross-slope at zero and taking flow sampler measurements in the central portion of the channel, where lateral shear could be neglected. For several trials, it was found that $n = 0.0104$.

Experimental flow distributions were measured with channel slopes from 1 to 6 percent

TABLE A
MINIMUM DEPTHS FOR FULLY DEVELOPED TURBULENT FLOW ON A CONCRETE SURFACE (n = .0104)

Longitudinal slope, %	Minimum depth, ft.
1	.070
2	.055
3	.035
4	.025
5	.020
6	—

[1] Larson, Curtis L., "Transverse Distribution of Velocity and Discharge for Flow in a Shallow Triangular Channel." Unpublished M.S. thesis, University of Minnesota, 1949. University of Minnesota Library.

[2] Larson, Curtis L., "Grate Inlets for Surface Drainage of Streets and Highways," Bulletin No. 2, St. Anthony Falls Hydraulic Laboratory, University of Minnesota, June 1949.

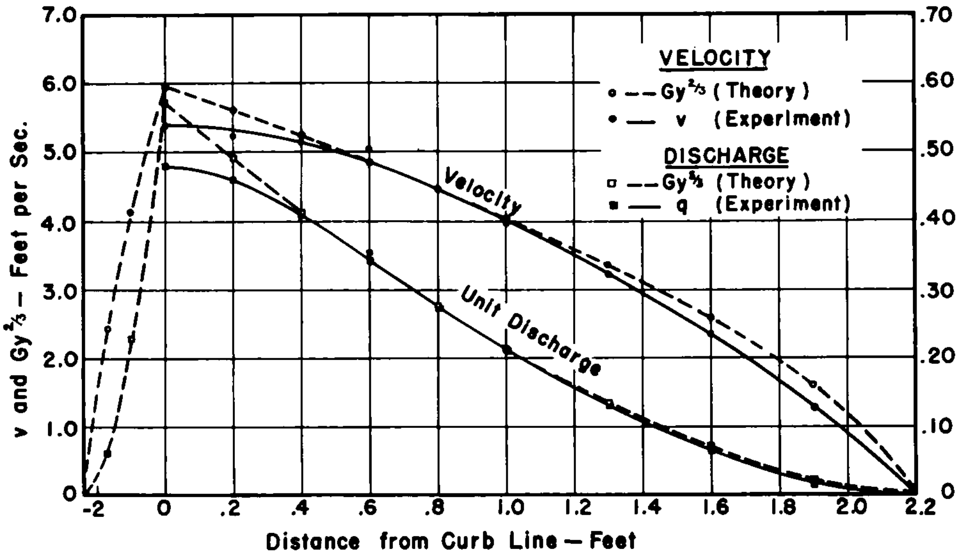

Figure A. Distribution of velocity and discharge for a cross slope of 20 to 1 and a longitudinal slope of 4%. Q = 0.523 cfs.

and with cross-slopes from 10:1 to 80:1. The validity of Eq. (1) was first tested by making a logarithmic plot of values of v vs. values of y for all tests, excluding all readings near the curb. This plot shows that Eq. (1), using $n = 0.0104$, held very well except for the flatter slopes and shallower depths. Minimum depths for which the equation proved suitable are given in Table A. It was concluded that fully developed turbulent flow was lacking with slopes of 1 and 2 percent except for a small part of the cross-section. For this reason, distribution data were presented only for longitudinal slopes of 3 to 6 percent.

Distributions of velocity and discharge for a typical test, both by theory and experiment, are presented in Figure A. For this slope, using $n = .0104$, G has a value of 28.58. In comparing the two velocity distributions, it will be noted that agreement is good in the central portion of the channel. Considerable discrepancy is evident in the left hand portion because of lateral shear from the curb. A noticeable difference is also present in the right hand portion, undoubtedly due to the shallow depths and partially developed turbulence in this area.

Theoretical discharge distributions were computed in a similar manner. As a two-dimensional discharge equation, the Manning equation is

$$q = Gy^{5/3} \tag{2}$$

where q is the discharge per unit width. Here again the experimental values are considerably lower than the theoretical quantities in the vicinity of the curb line. However, good agreement is obtained for the remainder of the channel, including the shallow portion. Although the percentage error in this area is the same as for the velocity distribution, the discharge here is so low that the absolute error can be considered negligible.

G. S. Tapley, *Closure*—The writer wishes to thank Professor Larson for his discussion. Like Larson, the writer first tested the approximate validity of Equation 7 by making logarithmic plots.

Although Larson's results agree in general with the writer's, one point of dissimilarity may be noted: Larson's theoretical velocities were greater than the experimental ones in the right hand portion of his cross section, whereas the opposite was true in the writer's case (Fig. 5). Factors which may explain the disparity are: Larson's channel was triangular in shape, while the writer's experimental channel had a bottom of parabolic cross section; Larson's theoretical velocities depended on the value of n, which he calculated for the point of maximum velocity, while the ordinates representing v/G in Fig. 5 are independent of n; they depend only on the slopes of the cumulative Q curve and the depths, in the experimental case, and on the depths alone in the theoretical one. The method employing scaled slopes from the cumulative Q curve involves inaccuracy of scaling, but otherwise is theoretically exact; it involves no systematic error such as is present when the velocity at the center of a finite element of cross section is taken to be the increment of discharge divided by the increment of area.

With regard to the minimum depths for turbulent flow, mentioned by Larson and listed in his Table 1, the writer had concluded that in his own case turbulent flow existed practically throughout the experimental range. This is evident from Table A where the values of Reynold's number, vy/ν, representing moderately low values of v and y from the experimental range are well above the value 500, above which turbulent flow may occur in open channels*.

TABLE A

S	$\nu \times 10^6$	y	v	vy/ν
0.005	10.5	0.0205	0.976	1,900
0.01	12.3	0.0173	1.153	1,630
0.02	10.5	0.0128	1.56	1,900
0.09	10.5	0.0076	2.62	1,900

In conclusion, it is believed that Equations 15 and 7 offer simple means for obtaining approximate velocity distributions for streets and similar channels.

* Engineering Hydraulics, Rouse, p. 83.

Stress Analysis and Design of Columns: A General Solution to the Compression Member Problem

Henson K. Stephenson, *Research Engineer,*
Texas Engineering Experiment Station

Oddly enough, in spite of the voluminous literature on the subject of columns, no method has been presented for actually analyzing the stresses in a practical compression member with restrained ends and centrally applied end loads, which also may or may not be subjected to certain superimposed angular end rotations. To contribute toward the realization of these needs a mathematical solution to the general compression member problem is developed and presented. The general solution is based on the fundamental concept that some degree of initial crookedness in the axis of a compression member is inherent in the column problem. The method presented for analyzing stresses results in a general solution that not only covers any degree of initial curvature or crookedness but also allows for the stress effects resulting from all possible combinations of end loading conditions. These include: fixed ends, restrained ends, equal or unequal end moments, angular rotation of the ends, and equal or unequal loading eccentricities. This general solution includes, as special cases, the formulas for pin ended members with unequal loading eccentricities developed and published (ASCE Trans. 1936) by D. H. Young and the secant formula for pin ended members with equal end loading eccentricities developed and published (1858) by H. Scheffler. The paper also includes several numerical examples and a number of tables and charts for use in the stress analysis and design of practical columns and other compression members.